

Simulation on Harmful Gas Control by Balanced Pressure Ventilation in the Fully Mechanized Caving Face under Sealed Fire Area of Small Coal Mine

Chaojun Fan, Hao Sun, Lei Yang,* Bin Xiao, and Lingjin Xu



Cite This: *ACS Omega* 2024, 9, 16168–16175



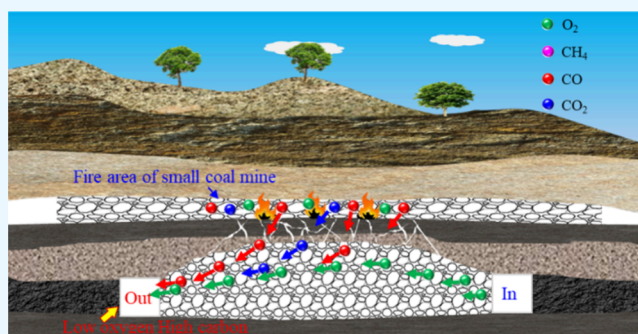
Read Online

ACCESS |

Metrics & More

Article Recommendations

ABSTRACT: The harmful gas in the sealed fire area of a small coal mine rushes into the mining face of the lower coal seam, which restricts the efficient promotion of the working face. In this paper, based on the evolution law of caving coal rock dilatation coefficient, the characteristics of the heterogeneous distribution of permeability and voidage in goaf were obtained, and the mathematical model of gas migration in goaf is constructed. The numerical solution of gas migration in goaf under the sealed fire area of a small coal mine was realized by using the Free and Porous Media Flow module and the Transport of Dilute Matter in Porous Media module in COMSOL Multiphysics, and the corresponding measure was proposed. The results show that the fresh air flows into the goaf from both the inlet air roadway and the working face and then flows out from the upper corner. Driven by the air flow, the CO in the overlying sealed fire area of a small coal mine flows out from the upper corner of the working face, resulting in the CO overlimit. Due to the influence of air leakage and the CO overlimit in the working face, low oxygen occurs in the working face. According to the characteristics of gas emission, balanced pressure ventilation technology is proposed to control the low oxygen in the working face and the CO overlimit in the upper corner. It is found that the balanced pressure ventilation obviously increases the pressure of the working face, reduces the pressure difference between the two ends of the working face by 45.7–26.7%, and decreases the air leakage to the goaf in the upper corner of the inlet air roadway. The field application shows that the problems of low oxygen in the working face and a CO overlimit in the upper corner are effectively solved.



1. INTRODUCTION

Most of coal mines are mined underground in China, and the spontaneous combustion fires in the airspace are one of the main challenges to the safe and efficient advancement of the working faces.^{1,2} The spontaneous combustion of residual coal in goaf will produce a large amount of toxic and harmful gases such as CO. These harmful gases migrate to the working face under the action of concentration difference and air flow in the goaf, which is easy to cause asphyxiation casualties.^{3–5} When it comes to the spontaneous combustion of goaf, it is difficult to control the spontaneous combustion of the overlying goaf, especially when there is a sealed fire area of small coal mine above the coal seam, as shown in Figure 1.⁶ Due to the lack of corresponding information and the difficulty in sealing the air leakage, it brought high safety risks to the advancement of the working face.⁷ Therefore, the development of appropriate ventilation technology for the characteristics of gas emergence under the sealed fire area of small coal mine is the key to safe mining.⁸

To prevent the spontaneous combustion of residual coal in goaf from threatening the working faces, the migration law of

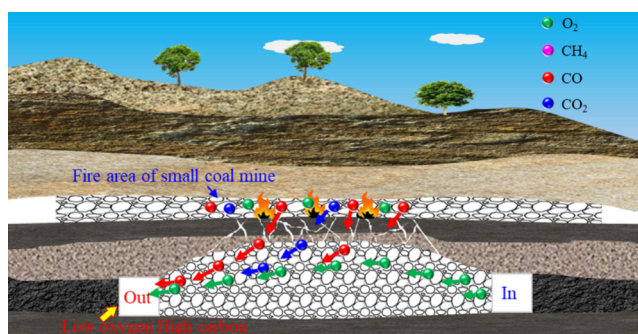


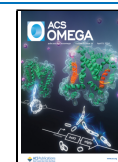
Figure 1. Schematic diagram of the impact of the sealed fire area of a small coal mine on the overlying working face.

Received: December 19, 2023

Revised: March 8, 2024

Accepted: March 14, 2024

Published: March 29, 2024



harmful gases in goaf should be clarified first. In order to more closely match the environment of spontaneous combustion of residual coal in goaf, experimental furnaces of different scales were developed and used to simulate the spontaneous combustion pattern of coal.^{9,10} Compared with the small experimental equipment, the coal samples in the large experimental furnace are more suitable for the coal sample size in the field, but its cost is higher and the experiment period is longer.^{11,12} Through these experimental devices, it is possible to monitor the change pattern of each characteristic parameter in the process of the spontaneous combustion of coal. For example, the diffusion rate of O₂ at the inlet air side of the goaf is obviously more rapid than that at the return air side, especially if the inlet air velocity is high.¹³ When the temperature in goaf increases gradually, the concentration of CO and C₂H₄ gas also presents a corresponding increase, with the ratio of CO/CO₂ increasing exponentially. When the O₂ concentration becomes low, the ignition point of coal gradually increases and the ignition time is delayed obviously.^{14,15} The amount of air leakage is positively correlated with the intensity of spontaneous combustion of coal and negatively correlated with the scope of harmful gas aggregation, and the scope of spontaneous combustion of coal increases when the air inlet velocity is higher.¹⁶ In response to the disaster of spontaneous combustion of coal, scholars have studied the suppression for the spontaneous combustion of coal by different means through experiments, such as the injection of inert gas, the three-phase foam fire protection, the sand suspension colloid fire protection, the spherical ice capsules filled with liquid nitrogen to extinguish fires, and so on.^{17–20} Although experimental studies can obtain some laws, they cannot present the real working conditions completely due to the influence of scale. The computational fluid dynamics (CFD) is more helpful to study the mechanism of fluid migration in the goaf. Porosity is a key factor affecting permeability, air leakage, and fluid migration in coal seams as well as simulating fluid migration in goaf. During the advancement of the working face, the cracks in the overlying rock strata continue to develop upward, and the porosity in the center of the goaf decreases while increasing near the working face and the ends of the coal seam.^{21,22} On this basis, it is found through simulation that the closer it reaches to the top, the wider the diffusion range of O₂ concentration becomes.²¹ When the air intake or porosity is large, the temperature is more likely to rise and the coal is more likely to spontaneously combust.²³ With the increase of air intake, the high temperature point of the goaf warms up, resulting in the acceleration of the migration rate of CO and other gases, and the high temperature area moves to the deeper part of the goaf, which is not conducive to the control of coal spontaneous combustion.²⁴ As the spontaneous combustion of coal consumes large amounts of O₂, the hazard area on gas explosion is shrinking, but the danger is increasing.²⁵ The area of the oxidation zone in the goaf reduced by 25% after the injection of inert gas.^{26,27} All of the above studies provide important references for the spontaneous combustion disaster of coal in the goaf, but there are few studies on the migration law of harmful gases in the working face under the sealed fire area of a small coal mine. In order to solve the problem of low oxygen and excessive harmful gas in the working face caused by air leakage under the sealed fire area of a small coal mine. It is necessary to clarify the migration law of harmful gas and change the flow direction of harmful gas from the root, so as to

ensure safe and efficient mining of the working face under the sealed fire area of a small coal mine.

This paper takes the 13102 working face of Shaping Mine as the research background by constructing a mathematical model of gas migration in the goaf and inverting the gas migration process of the 13102 working face by using the Free and Porous Media Flow module and the Transport of Dilute Matter in Porous Media module in COMSOL Multiphysics. On this basis, it is proposed to adopt balanced pressure ventilation technology to solve the problem of low oxygen and CO overlimit in the working face, in order to provide a reference for other similar working conditions.

2. MATHEMATICAL MODEL OF GAS MIGRATION IN GOAF

2.1. Momentum Conservation Equation of Gas Migration. The coal rock fracture field after mining belongs to a porous medium, and the migration of O₂, CO, and other gases in the mining fracture field satisfies the law of conservation of momentum. The Reynolds number of Darcy flow is 1–10, the Reynolds number of pipeline flow is generally greater than 2300, and the Reynolds number of air flow in goaf is less than 200. Therefore, the gas migration is between the pipe flow and the Darcy flow.

The Brinkman equation can describe the fluid flowing rapidly in porous media, and its kinetic energy comes from the velocity, pressure, and gravity of the fluid driving the flow. This equation extends Darcy's law to describe the kinetic energy dissipation caused by viscous shear. Therefore, Brinkman is very suitable for simulating the fast flow in porous media, including the transition between the slow flow in porous media controlled by Darcy's law and the fast flow described by Navier–Stokes equations. The Brinkman interface can simultaneously calculate the velocity and pressure of both. The expression of the equation is²⁸

$$\frac{\rho}{\varepsilon} \frac{\partial u}{\partial t} + \frac{\mu}{k} u = -\nabla p + \nabla \left(\frac{\mu}{\varepsilon} (\nabla u + (\nabla u)^T) \right) + F \quad (1)$$

where u is the fluid migration velocity, m/s; ρ is the underground air density, kg/m³; ε is the voidage of coal and rock mass; k is the permeability of coal and rock, m²; μ is the dynamic viscosity of downhole air, Pa·s; p is the pressure of fluid, Pa; F is the external volume force, $F = (\rho_0 - \rho)g$, N/m³; ρ_0 is the mixed gas density of CH₄, CO, and air, kg/m³.

2.2. Governing Equation of Gas Concentration Field. The migration of CO and O₂ in goaf also follows Fick's diffusion law and the hydrodynamic dispersion law. The gas diffusion in the mining fissure field can be described by the convection-diffusion equation in porous media. The sum of the rate of change of gas with time, the diffusion term, and the convective term is equal to the relative emission velocity of gas:²⁹

$$\theta_s \frac{\partial c_i}{\partial t} + \nabla \cdot (-\theta_s D_L \nabla c_i + u c_i) = S_{c_i} \quad (2)$$

where θ_s is the fluid volume rate; c_i is the concentration of different gases, kg/m³; D_L is the pressure diffusion tensor, m²/d; S_{c_i} is the reaction term, referring to the increase of gas in coal rock per unit volume in a unit time, where it represents the relative emission rate of CO and O₂, mol/(m³·s).

2.3. Permeability of Caving Coal Rock in Goaf. The relationship between permeability and porosity in the postmining coal rock fracture field is

$$k = \frac{D_p^2}{150} \frac{\varepsilon^3}{(1 - \varepsilon)^2} \quad (3)$$

where D_p is the average particle diameter of caving coal rock in the goaf, m.

The relationship between the porosity and the dilatation coefficient is³⁰

$$\varepsilon = 1 - \frac{1}{K_p(x, y)} \quad (4)$$

where $K_p(x, y)$ is the distribution of dilatation coefficients of caving coal rock in the goaf.

Under the action of overburden stress, coal pillar, and working face support, the distribution characteristics of fissures in the mining area are different. The fractures are more developed near the roadway and the working face, while the caving coal rock behind the working face is gradually compacted as the working face moves forward. The evolution law of the fracture dilatation coefficient of the caving coal rock behind the working face is obtained as³¹

$$K_p(x, y) = K'_p + (K_p^0 - K'_p) \cdot e^{-a_x d_x \cdot (1 - e^{-a_y d_y})} \quad (5)$$

where K'_p is the dilatation coefficient of caving coal rock mass after compaction; K_p^0 is the initial dilatation coefficient of caving coal rock mass; a_x is the attenuation rate of coal rock mass dilatation coefficient in the goaf away from the working face, m^{-1} ; a_y is the attenuation rate of coal rock mass dilatation coefficient in the goaf away from the solid wall, m^{-1} ; d_x is the distance to working face, m; d_y is the distance to the solid wall, m; ξ_1 is the adjustment coefficient of the "O" ring pattern.

3. RESULTS AND DISCUSSION

3.1. Numerical Simulation Experiment Method.

COMSOL Multiphysics is based on a finite element method and realizes multiphysics coupling by solving partial differential equations. The Free and Porous Media Flow module in COMSOL Multiphysics is used to define the air flow in the working face. By solving the module, it can obtain the distribution of the pressure and velocity fields in the working face and the mining area after air flow equilibrium. The transport and diffusion of CH_4 , O_2 , and CO are described by the dilute matter transfer in porous media. By solving the free and porous media flow equations in conjunction with the equation for the dilute matter transfer in porous media, we can obtain the process of CH_4 and CO transport to the working face, as well as the evolution law of the gas volume fractions at each spatial location of the working face and the goaf.

3.1.1. Geological Background and Construction of the Geometric Model. The main coal seam of Shaping Mine is 13#, the thickness of which is 8–14 m, with an average coal thickness of 12 m. The goafs of the 8# and 9# coal seam of the original volcano coal mine and 8# gob of Nanzhenggou coal mine are overlying, which have the possibility of spontaneous combustion. Among them, the 13102 working face is mined by comprehensive mechanized top coal caving technology with one full seam large mining height. The length of pushing mining is 1651 m and the length of the working face is 180.5 m. The height of cutting coal is 4.3 m, and the height of

releasing coal is 7.9 m, with the ratio of mining and releasing of 1:1.8. The working face is arranged along the inclination of the coal seam with the adoption of U-shaped ventilation. According to the field measurement, the inlet air speed is 1.5 m/s. Before the mining of the 13102 working face, the radon method and the drilling hole detection were used to determine two abnormal areas in the middle of the cutting eye and tape transport roadway: within the cutting eye range, by using the drilling hole detection, it found the CO levels that were above 1000 ppm, without high temperature being detected. After analysis, it was determined that abnormal CO levels were caused by the presence of the Nanzhenggou Old coal mine in the overlying strata. In order to ensure the safe and efficient mining of the 13102 working face, the migration law of goaf gas during the mining process is analyzed by numerical simulation. In the geometric model, the y -axis direction is defined as the inclination of the working face, while the x -axis direction is defined as the advancing direction of the working face and the vertical direction is defined as the z -axis direction. A geometric model measuring 180.5 m \times 320 m \times 47 m is constructed, with the goaf of the 8# coal seam located 42 m above the 13102 working face, as shown in Figure 2. The

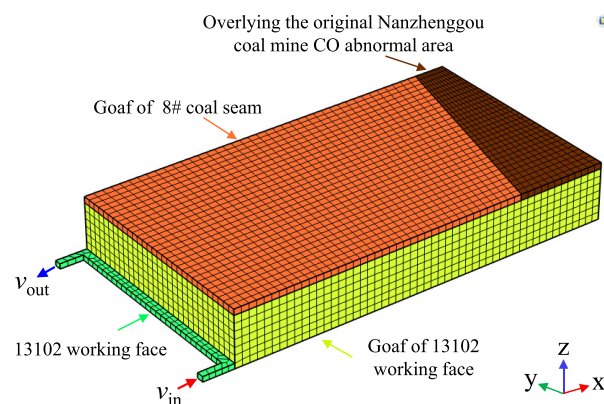


Figure 2. Geometric model of goaf in the 13102 working face.

geometric model was divided into hexahedral meshes, and the total number of elements was 12546, the minimum element mass was 0.4567, and the average element mass was 0.8096. The cross section of the intake airway is set as the velocity inlet boundary, the cross section of the return airway is set as the pressure outlet boundary, and the junction between the working face and the goaf is defined as the internal boundary. The boundary conditions of the model are shown in Table 1.

As the working face advances, the overlying strata of the coal seam are affected by mining-induced pressure, leading to the formation of a caving zone, fracture zone, and bending

Table 1. Simulation Boundary Condition of Gas Migration in Goaf under Small Kiln Fire Area

boundary and parameter	specific setting conditions
air intake	set to normal inflow velocity, wind speed is set to 1.5 m/s
air outlet	set the outlet relative pressure to 1 Pa to inhibit reflux
CO volume fraction	the CO volume fraction of high concentration was 20%
O_2 volume fraction	the O_2 volume fraction of the working face is set to 21%, and the O_2 volume fraction of the goaf is set to 0.5%

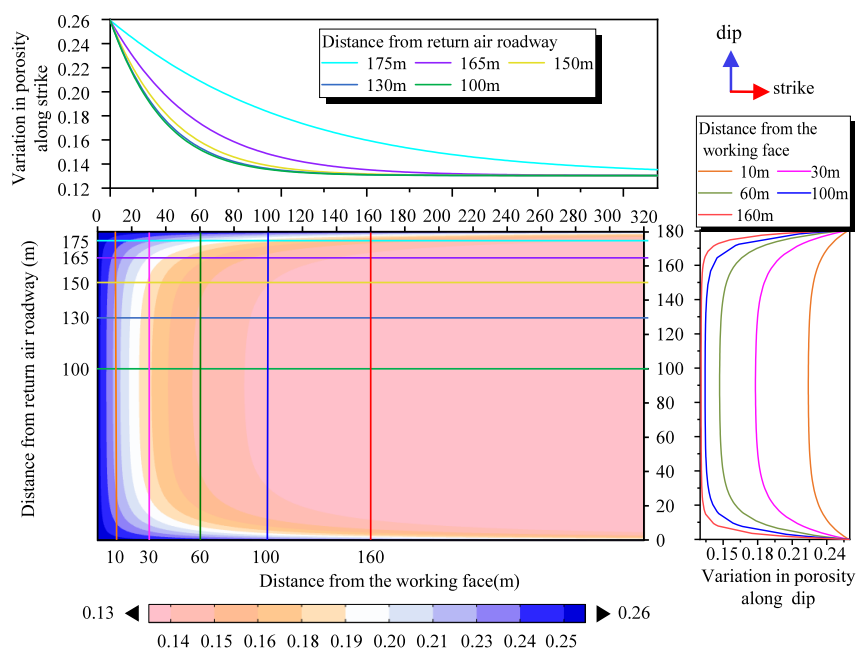


Figure 3. Permeability distribution of the simulated goaf.

Table 2. Simulation Parameters of Gas Migration in Goaf under Sealed Fire Area of Small Coal Mine

parameter	value	parameter	value
initial dilatation coefficient of caving coal rock mass (K_p^0)	1.35	attenuation rate of coal rock mass dilatation coefficient in the goaf away from the working face (a_w, m^{-1})	0.0368
dilatation coefficient of caving coal rock mass after compaction (K_p')	1.15	attenuation rate of coal rock mass dilatation coefficient in the goaf away from the solid wall (a_w', m^{-1})	0.268
average particle diameter of caving coal rock in the goaf (D_p, m)	0.05	adjustment coefficient of the "O" ring pattern (ξ_1)	0.233
dynamic viscosity of downhole air ($\mu, Pa \cdot s$)	1.84×10^{-5}	underground air density ($\rho, kg/m^3$)	1.29

subsidence zone. The collapsed rocks and remaining coal blocks within the caving zone will form a void space with specific structures as the working face advances. This spatial characteristic exhibits a certain heterogeneity. Based on eq 4, the distribution of void space in the goaf can be determined, allowing for the characterization of the porosity distribution in the goaf of 13102. Figure 3 illustrates the distribution of the porosity on the cross section at $z = 2$ m. In the vicinity of the working face, the support of the working face and the coal pillars provides a support to the back roof, resulting in the roof not completely collapsing and the coal-rock mass not being fully compacted, leading to a relatively large porosity. In the deeper part of the goaf, the fallen coal-rock mass is completely compacted, resulting in a smaller porosity. Permeability is an important parameter that characterizes fluid flow in the coal-rock mass. There is a certain correlation between the permeability and the porosity of the goaf. According to eq 3, the distribution of permeability in the goaf of the 13102 working face can be determined. The relevant parameters used in the numerical simulation process are shown in Table 2.

3.1.2. Evolution of Gas Migration in Goaf under Sealed Fire Area of Small Coal Mine. From Figure 4, it can be observed that during the process of O_2 entering the working face from the intake roadway, a portion of it leaks into the deeper part of the goaf through the intake upper corner, while some flow back toward the return upper corner with the return airflow. This is because at the interface between the goaf and the working face, where the overlying strata have not

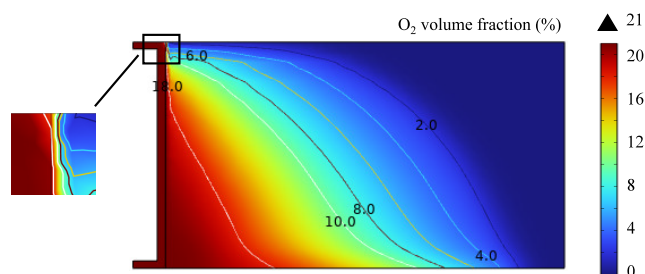


Figure 4. O_2 volume fraction evolution of goaf in the 13102 working face.

completely collapsed, the porosity and permeability are relatively large, resulting in less obstruction to the airflow. According to Fick's diffusion law, the concentration difference between the inside and outside of the goaf will cause O_2 to diffuse from the intake upper corner to the deeper part of the goaf and the return upper corner. During this process, O_2 will be consumed, resulting in a lower O_2 volume fraction in the deeper part of the goaf. Due to air leakage, the O_2 volume fraction at the return upper corner is lower ($<18\%$), leading to a low oxygen phenomenon.

Figure 5 shows the O_2 volume fraction at the intake side, middle, and return side of the goaf, which are perpendicular to the working face. The O_2 volume fraction follows the distribution pattern of low concentration near the working face and high concentration away from the working face on the intake side, middle, and return side. The volume fraction of the

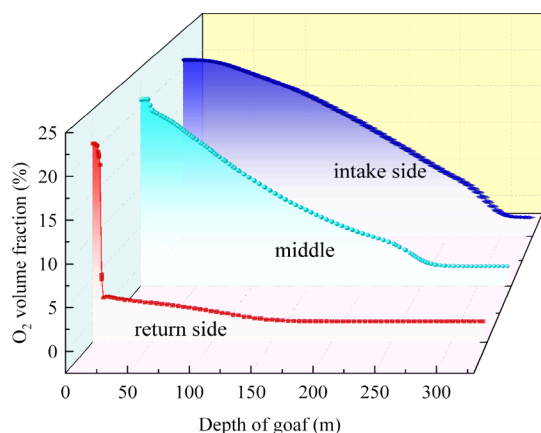


Figure 5. O₂ volume fraction at the intake side, middle, and return side of the goaf.

aqueous O₂ gradually increases from the intake side to the return side. At the deeper part of the goaf, the O₂ gradually dissipates, and the volume fraction decreases to zero.

The distribution pattern of the CO volume fraction is inversely related to that of the O₂ volume fraction, as shown in Figure 6. In the regions with a high volume fraction of O₂, the CO volume fraction is low. As the airflow progresses, CO gradually diffuses toward the return upper corner, resulting in a higher CO volume fraction in the area where the airflow exits. At the return upper corner, the CO volume fraction exceeds 24 ppm, posing a risk to the safe mining operations of the 13102 working face.

Figure 7 shows the CO volume fraction at the intake side, middle, and return side of the goaf, which are perpendicular to the working face. It can be observed that the CO volume fraction is higher at the return side compared to those at the intake side and middle. This is because the return airflow carries CO with a higher volume fraction to the return side, resulting in an increasing CO volume fraction at the return side. Based on the analysis above, it can be inferred that the 13102 working face may experience low oxygen and excessive CO levels during the mining process.

3.2. Application of Balanced Pressure Ventilation in Controlling Harmful Gases in Goaf. The balanced pressure ventilation technology involves taking measures to increase or decrease the air pressure in the working face so as to alter the leakage status of the goaf and control the airflow to prevent spontaneous combustion of residual coal and the accumulation of harmful gases in the working face. According to the characteristics of outburst during the mining process in the

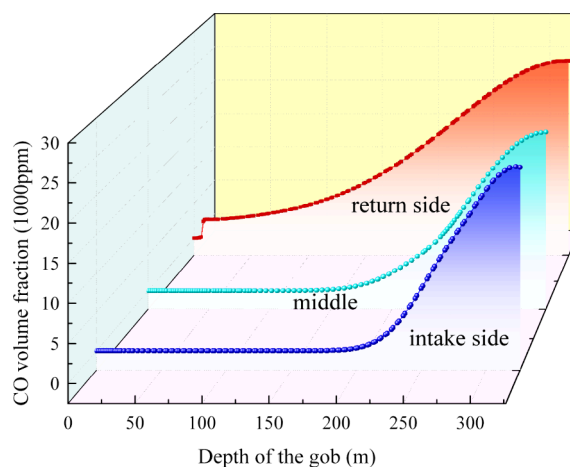


Figure 7. CO volume fraction at air inlet side, middle side, and return side of goaf.

13102 working face, the application of balanced pressure ventilation technology is proposed to address the issues of low oxygen and excessive CO levels in the working face during the mining process. This section will validate the feasibility of applying balanced pressure ventilation in the 13102 working face through numerical simulations. The boundary conditions for balanced pressure ventilation are that before balanced pressure ventilation, the airflow velocity in the intake roadway is 2.5 m/s, and the relative pressure at the exit of the return roadway is 1 Pa. After balanced pressure ventilation, the airflow velocity in the intake roadway and of the local ventilation fan is 1.2 and 0.4 m/s, respectively. The airflow resistance at the air window of the return roadway is increased by 10 Pa, and the relative pressure at the exit is 11 Pa.

3.2.1. Static Pressure Analysis before and after Implementing Balanced Pressure Ventilation. Figure 8 shows the distribution of relative static pressure at both ends of the working face before and after the implementation of balanced pressure ventilation. The pressure of the working face has been effectively increased after implementing balanced pressure ventilation. Before balanced pressure ventilation, the relative pressure at the upper corner of the intake roadway is approximately 12.5–11.5 Pa, and the relative pressure at the upper corner of the return roadway is approximately 4.4–5.5 Pa. The relative pressure difference between the two ends of the working face is approximately 8.1–6 Pa. After implementing balanced pressure ventilation, the relative pressure at the upper corner of the intake roadway is approximately 18.2–17.5 Pa, and the relative pressure at the upper corner of the return

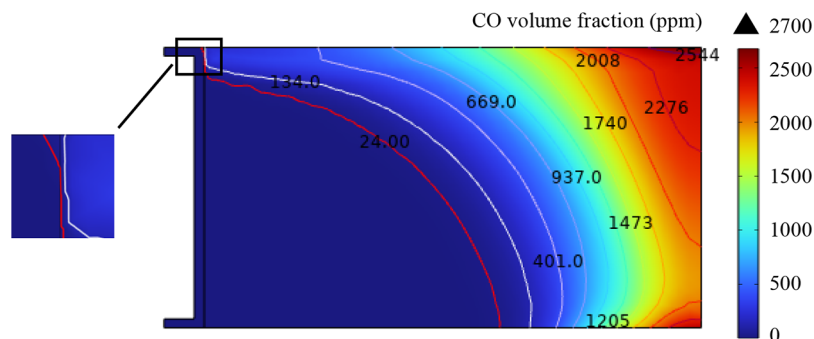


Figure 6. CO volume fraction evolution of goaf in 13102 working face.

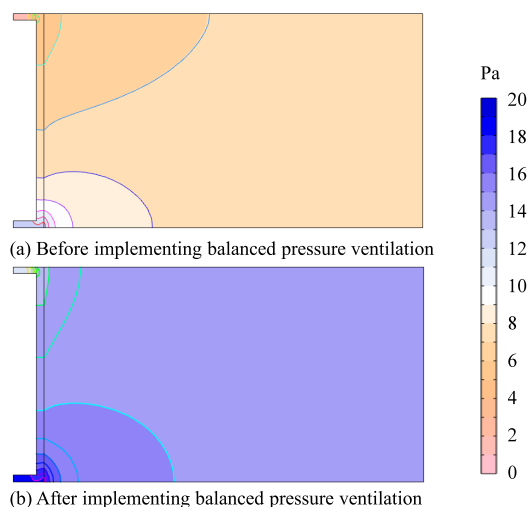


Figure 8. Static pressure distribution before and after the implementation of balanced pressure ventilation.

roadway is approximately 13.8–13.1 Pa. The pressure difference between the two ends of the working face is approximately 4.4 Pa. After implementing balanced pressure ventilation, the pressure difference between the two ends of the working face has decreased by approximately 3.7–1.6 Pa, with a reduction of around 45.7 to 26.7%. The balanced pressure ventilation greatly increases the pressure of the working face, reduces the pressure difference between the two ends, and effectively inhibits the air leakage of the working face.

3.2.2. Distribution of O_2 Volume Fraction. As shown in Figure 9, the range of spreading of O_2 to the deep part of the

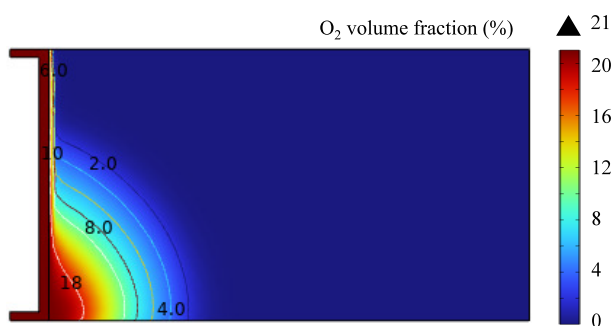


Figure 9. Distribution of the O_2 volume fraction under balanced pressure ventilation.

goaf obviously reduces under the condition of balanced pressure ventilation. The implementation of the balanced pressure ventilation technology not only reduces the pressure difference at both ends of the working face but also raises the pressure of the working face, which effectively reduces air leakage, increases the O_2 volume fraction of the working face, and effectively prevents the problem of low oxygen in the working face.

The O_2 volume fractions at the intake side, middle, and return side of the goaf are shown in Figure 10. The closer the goaf is to the inlet side, the higher the O_2 volume fraction is. The closer it is to the return side, the lower the O_2 volume fraction is. After the depth of the goaf exceeds 120 m, the O_2 volume fraction gradually decreases to zero. The balanced

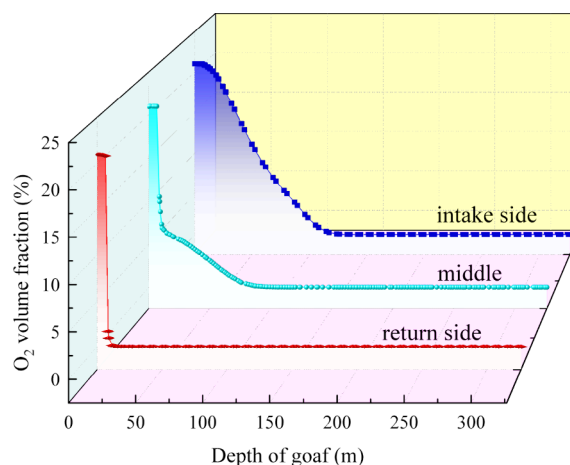


Figure 10. O_2 volume fractions at the intake side, middle, and return side of the goaf.

pressure ventilation technology effectively controls the diffusion of O_2 into the deep goaf.

3.2.3. Distribution of CO Volume Fraction. When no measures are taken for U-shaped ventilation, CO is driven by leakage air flow to surge rapidly into the return air side. Under the condition of balanced pressure ventilation, CO in the goaf uniformly diffuses toward the working face and is obviously separated from the working face, as shown in Figure 11. Due to

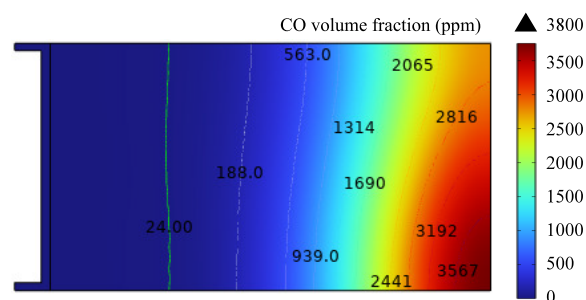


Figure 11. Distribution of the CO volume fraction under balanced pressure ventilation.

the combined pressure regulation, the air leakage volume decreases and the pressure difference between the two ends of the working face reduces, which inhibits the flow of CO from the overlying CO in the goaf to the upper corner of the working face and effectively prevents CO from gathering, as well as eliminates the safety hazard of CO exceeding the limit in the upper corner.

The changes of the CO volume fractions on the air inlet side, middle side, and return side of the goaf are shown in Figure 12. Corresponding to the cloud image, the CO volume fractions on the air inlet side, middle side, and return side of the goaf uniformly diffuse toward the working face due to the pressure difference. In the range of 75 m from the working face, the CO volume fraction is zero, and the problem of CO overlimit in the process of advancing the working face is effectively solved by the balanced pressure ventilation.

3.2.4. Field Application of Balanced Pressure Ventilation Technology. The emergency dynamic pressure regulation system of 13102 fully mechanized caving face is composed of the emergency dynamic pressure regulation fan installed in the room of the pressure regulator, the emergency dynamic

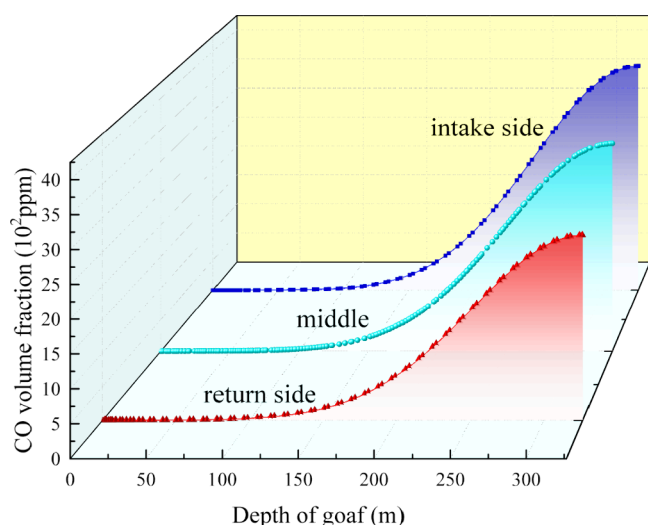


Figure 12. CO volume fraction at the air inlet side, middle side, and return side of the goaf under balanced pressure ventilation.

pressure regulation damper of the belt transportation roadway, the pedestrian damper of the belt transportation roadway (the main transportation roadway), and the emergency dynamic pressure regulation damper of the auxiliary transportation roadway. After the balanced pressure ventilation system is started, the adjustment of the emergency dynamic pressure regulating air door window of the main roadway is transported by tape and the pressure of the working face is raised to achieve the pressure balance of the overlying goaf and control the harmful gas from leaking down.

The CO and O₂ volume fractions at the corner of the 13102 fully mechanized caving face under the condition of balanced pressure ventilation are monitored. The monitoring data for 30 days are taken as shown in Figure 13. During the period, the

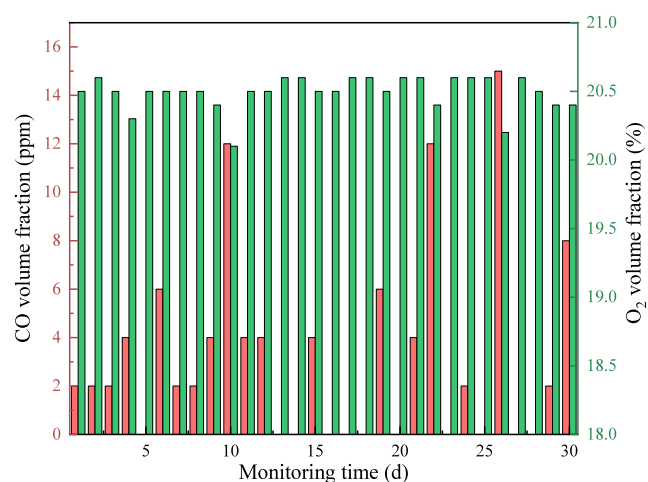


Figure 13. Change of the CO and the O₂ volume fraction at the upper corner of the return air roadway.

CO volume fraction fluctuates greatly but stabilizes below 24 ppm. The change of O₂ volume fraction is relatively stable, roughly distributed in about 20.5%, which effectively solves the problem of low oxygen in the working face and CO overlimit in the upper corner.

4. CONCLUSIONS

- (1) Based on the evolution law of the caving coal rock dilatation coefficient, the characteristics of the heterogeneous distribution of permeability and porosity in goaf were obtained. The mathematical model of gas migration in goaf was constructed. The numerical solution of gas migration in goaf under the sealed fire area of a small coal mine was realized by using the Free and Porous Media Flow module and the Transport of Dilute Matter in Porous Media module in COMSOL Multiphysics.
- (2) Fresh air flows into the goaf from the inlet roadway and working face and then flows out from the upper corner. Driven by the air flow, CO flows out from the upper corner of the working face in the overlying sealed fire area of a small coal mine, resulting in a CO overlimit. Due to the influence of air leakage in the working face, the CO concentration in the upper corner of the return air roadway is greater than 24 ppm and the O₂ concentration is less than 18%, which seriously threatens the production of the working face.
- (3) The balanced pressure ventilation technology is proposed to control the low oxygen and CO overlimit in the working face. The balanced pressure ventilation can not only increase the pressure of the working face but also reduce the pressure difference at both ends of the working face, as well as decrease the air leakage to the goaf in the upper corner of the inlet air roadway. After implementing balanced pressure ventilation, the CO volume fraction in the upper corner of the return air roadway is stable at less than 24 ppm, and the O₂ volume fraction is stable at about 20.5%, which can effectively solve the problem of low oxygen in the working face and CO overlimit in the upper corner.

AUTHOR INFORMATION

Corresponding Author

Lei Yang – College of Mining, Liaoning Technical University, Fuxin 123000, China; orcid.org/0000-0003-0692-5832; Email: leiyang106@163.com

Authors

Chaojun Fan – College of Mining, Liaoning Technical University, Fuxin 123000, China; orcid.org/0000-0003-4578-0760

Hao Sun – College of Mining, Liaoning Technical University, Fuxin 123000, China

Bin Xiao – College of Mining, Liaoning Technical University, Fuxin 123000, China; orcid.org/0000-0003-1006-7965

Lingjin Xu – College of Mining, Liaoning Technical University, Fuxin 123000, China

Complete contact information is available at:

<https://pubs.acs.org/10.1021/acsomega.3c10149>

Notes

The authors declare no competing financial interest.

Biographies

Chaojun Fan has a Ph.D. and is an associate professor at Liaoning Technical University. The research fields are multifield coupling law of energy/disaster fluid transport in fractured coal rock mass, involving the coal and gas outburst mechanism, enhanced gas (coalbed methane) extraction, and CO₂ geological storage.

Hao Sun is a graduate student at Liaoning Technical University. The research field is mine safety disaster prevention and control.

Lei Yang is a graduate student at Liaoning Technical University. The research field is gas-enhanced extraction and CO₂ sequestration.

Bin Xiao has a Ph.D. and is a lecturer at Liaoning Technical University. The research fields are exploration and evaluation of oil and gas resources and sedimentary tectonic pattern of shale layer.

Lingjin Xu is a graduate student at Liaoning Technical University. The research field is mine safety disaster prevention and control.

ACKNOWLEDGMENTS

This research was financially supported by the National Natural Science Foundation of China (grant nos. 52004117, 52174117, and 52074146), the Postdoctoral Science Foundation of China (grant nos. 2021T140290 and 2020M680975), the Discipline Innovation Team of Liaoning Technical University (grant no. LNTU20TD-03), and the Research Fund of State and Local Joint Engineering Laboratory for Gas Drainage & Ground Control of Deep Mines (Henan Polytechnic University) (SJF2205).

REFERENCES

- (1) Yang, L.; Fan, C.; Wen, H.; et al. An improved gas–liquid–solid coupling model with plastic failure for hydraulic flushing in gassy coal seam and application in borehole arrangement. *Phys. Fluids* **2023**, *35* (3), No. 036603.
- (2) Fan, C.; Yang, L.; Sun, H.; et al. Recent Advances and Perspectives of CO₂-Enhanced Coalbed Methane: Experimental, Modeling, and Technological Development[J]. *Energy Fuels* **2023**, *37* (5), 3371–3412.
- (3) Zhang, J.; Zhang, H.; Ren, T.; et al. Proactive inertisation in longwall goaf for coal spontaneous combustion control-A CFD approach[J]. *Safety science* **2019**, *113*, 445–460.
- (4) Lu, X.; Deng, J.; Xiao, Y.; et al. Recent progress and perspective on thermal-kinetic, heat and mass transportation of coal spontaneous combustion hazard[J]. *Fuel* **2022**, *308*, No. 121234.
- (5) Xia, T.; Zhou, F.; Wang, X.; et al. Controlling factors of symbiotic disaster between coal gas and spontaneous combustion in longwall mining gob[J]. *Fuel* **2016**, *182*, 886–896.
- (6) Xiao, B.; Xiong, L.; Zhao, Z.; et al. Late Ordovician-Early Silurian extension of the northern margin of the Upper Yangtze Platform (South China) and its impact on organic matter accumulation[J]. *J. Pet. Sci. Eng.* **2023**, *220*, No. 111238.
- (7) Fan, C.; Xu, L.; Elsworth, D.; et al. Spatial–Temporal Evolution and Countermeasures for Coal and Gas Outbursts Represented as a Dynamic System[J]. *Rock Mechanics and Rock Engineering* **2023**, *56* (9), 6855–6877.
- (8) Jayasuriya, J.; Moser, I.; de Mel, R. An automated water dispensing system for controlling fires in coal yards. *Int. J. Coal Sci. Technol.* **2022**, *9* (1), 23.
- (9) Wen, H. Experiment simulation of whole process on coal self-ignition and study of dynamical change rule in high-temperature zone. *Mei T'an Hsueh PaoJ. China Coal Soc.* **2004**, *29*.
- (10) Deng, J.; Xiao, Y.; Li, Q.; et al. Experimental studies of spontaneous combustion and anaerobic cooling of coal[J]. *Fuel* **2015**, *157*, 261–269.
- (11) Zhang, Y.; Zhang, Y.; Li, Y.; et al. Study on the characteristics of coal spontaneous combustion during the development and decaying processes[J]. *Process Safety and Environmental Protection* **2020**, *138*, 9–17.
- (12) Zhao, J.; Ming, H.; Guo, T.; et al. Semi-enclosed experimental system for coal spontaneous combustion for determining regional distribution of high-temperature zone of coal fire. *Int. J. Coal Sci. Technol.* **2022**, *9* (1), 62.
- (13) Zheng, Y.; Li, Q.; Zhang, G.; et al. Study on the coupling evolution of air and temperature field in coal mine goafs based on the similarity simulation experiments[J]. *Fuel* **2021**, *283*, No. 118905.
- (14) Ren, L. F.; Li, Q. W.; Xiao, Y.; et al. Critical parameters and risk evaluation index for spontaneous combustion of coal powder in high-temperature environment[J]. *Case Studies in Thermal Engineering* **2022**, *38*, No. 102331.
- (15) Xu, Y.; Liu, Z.; Wen, X.; et al. Effect mechanism of nitrogen injection into fire-sealed-zone on residual-coal re-ignition under stress in goaf. *Int. J. Coal Sci. Technol.* **2022**, *9* (1), 74.
- (16) Zheng, Y.; Li, Q.; Zhu, P.; et al. Study on multi-field evolution and influencing factors of coal spontaneous combustion in goaf[J]. *Combust. Sci. Technol.* **2023**, *195* (2), 247–264.
- (17) Lei, B.; He, B.; Xiao, B.; et al. Comparative study of single inert gas in confined space inhibiting open flame coal combustion[J]. *Fuel* **2020**, *265*, No. 116976.
- (18) Tian, Z. J.; Li, X. L. Research on technology for preventing spontaneous combustion of coal[J]. *Advanced Materials Research* **2012**, *524*, 677–680.
- (19) Xu, Y.; Wang, D.; Wang, L.; et al. Experimental research on inhibition performances of the sand-suspended colloid for coal spontaneous combustion[J]. *Safety science* **2012**, *50* (4), 822–827.
- (20) Torikai, H.; Ishidoya, M.; Ito, A. Examination of extinguishment method with liquid nitrogen packed in a spherical ice capsule[J]. *Fire Technol.* **2016**, *52*, 1179–1192.
- (21) Zhang, Y.; Niu, K.; Du, W.; et al. A method to identify coal spontaneous combustion-prone regions based on goaf flow field under dynamic porosity[J]. *Fuel* **2021**, *288*, No. 119690.
- (22) Zhu, H.; Liu, X. Theoretical investigation on the relationship between tail roadway methane drainage and distribution of easily spontaneous combustible region in gob. *Saf. Sci.* **2012**, *50* (4), 618–623.
- (23) Zhang, H.; Gao, E. 3D numerical simulation and influencing factors of loose top coal spontaneous combustion in roadway[J]. *International journal of heat and technology* **2015**, *33* (3), 91–96.
- (24) Wang, C.; Chen, L.; Bai, Z.; et al. Study on the dynamic evolution law of spontaneous coal combustion in high-temperature regions[J]. *Fuel* **2022**, *314*, No. 123036.
- (25) Zheng, Y.; Li, S.; Xue, S.; et al. Study on the evolution characteristics of coal spontaneous combustion and gas coupling disaster region in goaf[J]. *Fuel* **2023**, *349*, No. 128505.
- (26) Liu, Y.; Wen, H.; Guo, J.; et al. Coal spontaneous combustion and N₂ suppression in triple goafs: A numerical simulation and experimental study[J]. *Fuel* **2020**, *271*, No. 117625.
- (27) Zhao, P.; Zhuo, R.; Li, S.; et al. Greenhouse gas protection and control based upon the evolution of overburden fractures under coal mining: A review of methods, influencing factors, and techniques[J]. *Energy* **2023**, *284*, No. 129158.
- (28) Chen, X.; Shi, X.; Zhang, Y.; et al. Numerical simulation study on coal spontaneous combustion: Effect of porosity distribution[J]. *Combust. Sci. Technol.* **2023**, *195* (3), 472–493.
- (29) Zou, J.; Zhang, R.; Zhou, F.; et al. Hazardous area reconstruction and law analysis of coal spontaneous combustion and gas coupling disasters in goaf based on DEM-CFD[J]. *ACS Omega* **2023**, *8* (2), 2685–2697.
- (30) Qi, Y.; Wang, W.; Qi, Q.; et al. Distribution of spontaneous combustion three zones and optimization of nitrogen injection location in the goaf of a fully mechanized top coal caving face[J]. *PLoS One* **2021**, *16* (9), No. e0256911.
- (31) Wang, G.; Xu, H.; Wu, M.; et al. Porosity model and air leakage flow field simulation of goaf based on DEM-CFD. *Arabian J. Geosci.* **2018**, *11*, 1–17.